Inorganica Chimica Acta 485 (2019) 200–208

Contents lists available at ScienceDirect

Inorganica Chimica Acta

journal homepage: www.elsevier.com/locate/ica

Research paper

Synthetic, electrochemical, spectroscopic, and structural studies of mixed sandwich Co(III) complexes involving Cp or Cp* with tridentate N-donor and S-donor macrocycles

John P. Lee[a,*], Trevor P. Latendresse[a], Kristina R. Henson[a], Patrick A. Dean[a], Larry F. Mehne[b]

[a] The University of Tennessee at Chattanooga, Department of Chemistry & Physics, 615 McCallie Avenue, Chattanooga, TN 37403, USA
[b] Covenant College, Department of Chemistry, 14049 Scenic Highway, Lookout Mountain, GA 30750, USA

ARTICLE INFO

Keywords:
Cobalt complexes
1,4,7-Trithiacyclononane
1,4,7-Triazacyclononane
Mixed sandwich complexes
Macrocyclic ligands

ABSTRACT

The syntheses, structures, spectroscopy, and electrochemistry for four Co(III) mixed sandwich mononuclear complexes involving tridentate macrocycles and either cyclopentadienyl (Cp) or pentamethylcyclopentadienyl (Cp*) are reported. All complexes have the general formula $[Co(Cp^R)([9]aneX_3)](PF_6)_2$, where X = S, 1,4,7-trithiacyclononane, and R = Cp (**1**) or Cp* (**2**), or X = N, 1,4,7-triazacyclononane, and R = Cp (**3**) or Cp* (**4**), and exhibit a pseudo-octahedral structure involving the carbocyclic η^5-Cp^R ligand and facial κ^3-donation from the macrocycle. The structures for all six complexes are supported by ^1H and $^{13}C\{^1H\}$ NMR spectroscopy, and the compounds **1**, **2**, and **4** are also characterized by single-crystal X-ray crystallography. The ^1H NMR shows an AA′BB′ splitting pattern for the coordinated macrocycle, and the dispersion between the two sets of multiplets is dependent upon the identity of the macrocycle. The $[9]aneN_3$ complexes show only a single reversible (**4**) or irreversible (**3**) +3/+2 reduction in the −1.0 to −1.4 V range vs. Fc/Fc^+. The $[9]aneS_3$ complexes show the same reversible (**1**) or quasi-reversible (**2**) reduction in the −0.6 to −0.9 V range vs. Fc/Fc^+ as well as a quasi-reversible (**1**) or irreversible (**2**) +2/+1 reduction in the −1.5 to −1.8 V range vs. Fc/Fc^+.

1. Introduction

The coordination chemistry of the tridentate macrocycles 1,4,7-triazacyclononane ($[9]aneN_3$) and 1,4,7-trithiacyclononane ($[9]aneS_3$) has been an important focus of the inorganic and organometallic communities over the past 30 years [1–10]. More recent work with these types of macrocyclic ligands includes application to C—H bond activation and O_2 activation [9,11,12]. The two macrocycles can be compared to η^5-cyclopentadienyl anion and η^5-pentamethylcyclopentadienyl anion (Cp and Cp*, respectively), η^6-arenes (*e.g.*, *p*-cymene and hexamethylbenzene), and κ^3-hydrido-tris(pyrazolyl)borate (Tp) ligands in that all can occupy three facially coordinating sites. Mixed sandwich complexes containing $[9]aneS_3$ or $[9]aneN_3$ with other facially coordinating tridentate ligands have been synthesized with Group 8 and 9 d^6 metals by several research groups [13–22]. In addition, the mixed macrocycle sandwich complex $[Co([9]aneS_3)([9]aneN_3)](Br)_3$ has been reported [23]. Most germane to this work are the mixed sandwich complexes reported by Grant *et al.* that involve either Rh(III) or Ir(III) of the type $[M(Cp^*)(L)](PF_6)_2$, where L = $[9]aneS_3$, [10]$aneS_3$, and $[9]aneN_3$ [24]. Our current work expands the aforementioned examination of mixed sandwich complexes by synthesizing complexes of the type $[Co(Cp^R)([9]aneX_3)](PF_6)_2$, where X = S or N and R = Cp or Cp*, which completes the Group 9 metal triad specifically for $[M(Cp^*)([9]aneS_3)](PF_6)_2$ and $[M(Cp^*)([9]aneN_3)](PF_6)_2$.

Interest in Co(III) complexes with Cp or Cp* arises from the increased focus toward the development of homogeneous catalysts utilizing base metals [25,26], and the use of Cp* along with Rh(III) and Ir(III) has had great applicability in a variety of organometallic reactions [27–30]. Furthermore, complexes of the type $\{[Co^{III}(Cp^*)(L)_l]^{n+}\}$ have recently been utilized for catalytic carbon-hydrogen bond activation/carbon-carbon coupling reactions and transfer hydrogenation reactions [31–34]. Moreover, computational reports have suggested that $\{[Co(Cp^*)(PMe_3)(CH_3)]^{1+}\}$ would be of interest for catalytic carbon-hydrogen bond activation reactions such as methane C—H activation and oxy-functionalization of hydrocarbons [35,36].

Of additional interest is how the $[9]aneN_3$ and $[9]aneS_3$ will interact with the Co(III) ion. In general, $[9]aneN_3$ is a better σ-donor ligand that behaves as a hard-base while $[9]aneS_3$ has a π-accepting component and behaves as a soft-base [6,37]. Since the σ-donor/π-

* Corresponding author.
E-mail address: John-Lee@utc.edu (J.P. Lee).

https://doi.org/10.1016/j.ica.2018.08.058
Received 26 July 2018; Accepted 31 August 2018
Available online 05 October 2018
0020-1693/ © 2018 Elsevier B.V. All rights reserved.

acceptor (and hard/soft base) characteristics of [9]aneN$_3$ and [9]aneS$_3$ are very different the distinctions in their complexation properties in a mixed ligand environment will be of interest with the first-row transition metal, Co(III). Employing these two macrocycles, we wish to probe how the ligand differences will influence the structural, spectroscopic, and electrochemical properties for a series of heteroleptic Cp and Cp* complexes containing Co(III).

2. Experimental section

2.1. Materials

All solvents and reagents were used as received. The ligands [9]aneS$_3$, and [9]aneN$_3$·3HCl, as well as both silver hexafluorophosphate and tetra-*N*-butylammonium hexafluorophosphate were purchased from either Aldrich Chemical Company or Acros Organics and used as received. The metal reagents [Co(Cp)(CO)(I)$_2$] and [Co(Cp*)(CO)(I)$_2$] were prepared according to previously reported methods [38,39].

2.2. Measurements

^{1}H and ^{13}C{^{1}H} NMR spectra were obtained on a JEOL ECX 400 MHz spectrometer (operating frequency for ^{13}C NMR was 100 MHz) and referenced against tetramethylsilane using residual proton signals (^{1}H NMR) or the ^{13}C resonances of the deuterated solvent (^{13}C{^{1}H} NMR). ^{31}P{^{1}H} NMR spectra were obtained on a JEOL ECX 400 MHz (operating frequency = 161 MHz) spectrometer and referenced against external 85% H_3PO_4. Unless otherwise noted, NMR spectra were acquired at room temperature. UV-vis spectra were obtained on a Varian Cary UV-vis spectrophotometer in acetonitrile using 1 cm quartz cuvettes. Elemental analyses were performed by Atlantic Microlab, Inc in Norcross, GA. Electrochemical measurements were performed using a Bioanalytical Systems CV50W analyzer. The supporting electrolyte was 0.1 M [(Bu)$_4$N]BF$_4$ in CH_3CN, and sample concentrations ranged from 1 to 2 mM. All voltammograms were recorded at a scan rate of 100 mV/s over a −0.7 to +2.4 V (vs. Fc/Fc$^+$) window. The standard three electrode configuration was as follows: Pt disk working electrode, Pt-wire auxiliary electrode, and Ag/0.01 M Ag(I) reference electrode. All potentials are reported against the Fc/Fc$^+$ standard couple.

2.3. Syntheses

2.3.1. Preparation [Co(Cp)([9]aneS$_3$)](PF$_6$)$_2$ (1)

A 100 mL round-bottom flask was charged with [Co(Cp)(CO)(I)$_2$] (0.109 g, 0.267 mmol) and EtOH (50 mL). To the purple solution was added [9]aneS$_3$ (0.0542 g, 0.301 mmol), and the solution was heated to reflux under N$_2$ for 1.5 h. Upon completion of the reflux, [^{n}Bu$_4$N](PF$_6$) (0.260 g, 0.677 mmol) was added to the red solution and the system was refluxed for an additional 3 h, and was then left to stir at room temperature overnight. The next day, a precipitate had formed in the bottom of the flask, which was filtered and the solid was re-dissolved in nitromethane (~1 to 2 mL). An orange precipitate formed upon the addition of diethyl ether (~20 mL) which was collected by vacuum filtration and dried *in vacuo*. (0.089 g, 56% yield). ^{1}H NMR (CD_3NO_2,δ): 6.26 (5H, s, Cp C*H*), 3.49–3.18 (12H, m, [9]aneS$_3$ C*H*$_2$). ^{13}C{^{1}H} NMR (CD_3NO_2, δ): 93.9 (5C, s, Cp *C*H), 41.0 (6C, s, [9]aneS$_3$ *C*H$_2$). ^{31}P NMR (CD_3NO_2, δ): −145 (1P, m, *P*F$_6$). UV–Vis (acetonitrile, nm (ε/M^{-1} cm^{-1})): 432 (1.26×10^3), 363 (2.10×10^3), 305 (2.77×10^4), and 246 (2.57×10^4). Anal. Calcd for $C_{11}H_{17}CoF_{12}P_2S_3$: C, 22.23; H, 2.88; S, 16.19. Found: C, 22.94; H, 2.81; S, 16.30. Cyclic voltammetry shows one reversible one-electron reduction with $E^{\circ\prime} = -0.582$ V, $i_{pc}/i_{pa} = 1.198$, $\Delta E_p = 68$ mV and one quasi-reversible electron reduction with $E^{\circ\prime} = -1.524$ V, $i_{pc}/i_{pa} = 1.472$, $\Delta E_p = 68$ mV versus Fc/Fc$^+$ ($i_{pc}/i_{pa} = 0.924$ and $\Delta E_p = 68$ mV).

2.3.2. Preparation of [Co(Cp*)([9]aneS$_3$)](PF$_6$)$_2$ (2)

A 100 mL round-bottom flask was charged with [Co(Cp*)(CO)(I)$_2$] (0.104 g, 0.218 mmol) and EtOH (50 mL). To the purple solution was added [9]aneS$_3$ (0.0483 g, 0.268 mmol), and the solution was heated to reflux under N$_2$ for 1.5 h. Upon completion of the reflux, [^{n}Bu$_4$N](PF$_6$) (0.213 g, 0.550 mmol) was added and the resulting red solution was refluxed for an additional 3 h, and was then left to stir at room temperature overnight. The next day, a precipitate had formed in the bottom of the flask, which was filtered and the solid was re-dissolved in nitromethane (~1 to 2 mL). Addition of diethyl ether (~20 mL) gave rise to a cloudy solution, which was cooled for approximately 2 h to precipitate the yellow product. The product was collected by vacuum filtration and was dried *in vacuo*. (0.084 g, 58% yield). ^{1}H NMR (CD_3NO_2, δ): 3.34–3.16 (12H, m, [9]aneS$_3$ C*H*$_2$), 1.83 (15H, s, Cp* C*H*$_3$). ^{13}C{^{1}H} NMR (CD_3NO_2, δ): 105.2 (5C, s, Cp* *C*CH$_3$), 39.2 (6C, s, [9]aneS$_3$ *C*H$_2$), 10.3 (5C, s, Cp* *C*H$_3$). ^{31}P NMR (CD_3NO_2, δ): −144 (1P, m, *P*F$_6$). UV-Vis (acetonitrile, nm (ε/M^{-1} cm^{-1})): 440 (1.26×10^3), 366 (1.32×10^3), 300 (4.20×10^4). Anal. Calcd for $C_{16}H_{27}CoF_{12}P_2S_3$: C, 28.92; H, 4.10; S, 14.48. Found: C, 29.03; H, 4.08; S, 14.18. Cyclic voltammetry shows one quasi-reversible one-electron reduction with $E^{\circ\prime} = -0.872$ V, $i_{pc}/i_{pa} = 2.101$, $\Delta E_p = 68$ mV and one irreversible reduction with $E^{\circ\prime} = -1.837$ V, $i_{pc}/i_{pa} = 2.183$, $\Delta E_p = 178$ mV versus Fc/Fc$^+$ ($i_{pc}/i_{pa} = 0.938$ and $\Delta E_p = 68$ mV).

2.3.3. Preparation of [Co(Cp*)([9]aneS$_3$)](BF$_4$)$_2$ (2a)

A 100 mL round-bottom flask was charged with [Co(Cp*)(CO)(I)$_2$] (0.0598 g, 0.126 mmol) and nitromethane (50 mL). To the purple solution was added [9]aneS$_3$ (0.0282 g, 0.156 mmol), and the solution was heated to reflux under N$_2$ for 1.5 h. Upon completion of the reflux, the nitromethane was completely removed on a rotary evaporator and the residue was re-dissolved in a 1:1 (v/v) water/methanol mixture (50 mL). To that solution, NaBF$_4$ (0.0343 g, 0.313 mmol) was added and the solution refluxed for an additional 30 min. The solvent was completely removed by rotary evaporation and the residue was dissolved in nitromethane (~10 mL). A white precipitate had formed in the bottom of the flask, which was filtered through a celite plug leaving an orange solution. The filtrate was reduced to ~1 to 2 mL, and diethyl ether (~20 mL) was added to precipitate an orange product. The product was collected by vacuum filtration and was dried *in vacuo*. (0.0429 g, 62% yield). ^{1}H NMR (CD_3NO_2, δ): 3.29 (12H, s, [9]aneS$_3$ C*H*$_2$), 1.83 (15H, s, Cp* C*H*$_3$).

2.3.4. Preparation of [Co(Cp*)([9]aneS$_3$)](ClO$_4$)$_2$ (2b)

A 100 mL round-bottom flask was charged with [Co(Cp*)(CO)(I)$_2$] (0.103 g, 0.215 mmol) and nitromethane (50 mL). To the purple solution was added [9]aneS$_3$ (0.0469 g, 0.260 mmol), and the solution was heated to reflux under N$_2$ for 1.5 h. Upon completion of the reflux, NaClO$_4$ (0.0602 g, 0.149 mmol) was added and the resulting red solution was refluxed for an additional 30 min. A precipitate had formed in the bottom of the flask, which was removed by filtering the reaction mixture through a celite plug. The red filtrate was reduced to ~1 to 2 mL, and diethyl ether (~20 mL) was added to precipitate a red product. The product was collected by vacuum filtration and was dried *in vacuo*. (0.104 g, 84% yield). ^{1}H NMR (CD_3NO_2, δ): 3.35–3.22 (12H, m, [9]aneS$_3$ C*H*$_2$), 1.84 (15H, s, Cp* C*H*$_3$).

2.3.5. Preparation of [Co(Cp)([9]aneN$_3$)](PF$_6$)$_2$ (3)

A 100 mL round-bottom flask was charged with [9]aneN$_3$·3HCl (0.0739 g, 0.310 mmol) and EtOH (30 mL). To the mixture, 9.30 mL of dilute aqueous NaOH (0.1 M, 0.923 mmol) was added in 3 portions waiting 10–15 min between each addition. After the NaOH addition, the solution became homogeneous, and was slightly basic according to pH paper. To this solution, [Co(Cp)(CO)(I)$_2$] (0.0971 g, 0.239 mmol) was added and the orange mixture was heated to reflux under N$_2$ for 1.5 h. Once heated, the mixture became dark red and homogeneous. After cooling, AgPF$_6$ (0.128 g, 0.508 mmol) was added, giving rise

immediately to an orange precipitate. The mixture was heated to reflux for 30 min in the dark and then cooled to room temperature. Upon filtering through a celite plug, a burnt orange filtrate was recovered. The filtrate was reduced to dryness on the rotary evaporator and the residue was taken up in nitromethane (~20 mL). A white precipitate formed, and the mixture was filtered through a second celite plug. The filtrate was reduced to a minimum amount and a precipitate was formed upon addition of diethyl ether (~20 mL). The final orange-brown product was collected by vacuum filtration and was dried *in vacuo*. (0.044 g, 34% yield). ^{1}H NMR (CD_3NO_2, δ): 7.51 (3H, s, [9]aneN$_3$ N*H*) 5.89 (5H, s, Cp C*H*) 3.55–2.76 (12H, m, [9]aneN$_3$ C*H*$_2$). ^{13}C{^{1}H} NMR (CD_3NO_2, δ): 88.0 (5C, s, Cp *C*H), 53.7 (6C, s, [9]aneN$_3$ *C*H$_2$). ^{31}P NMR (CD_3NO_2, δ): −150 (1P, m, *P*F$_6$). UV–Vis (acetonitrile, nm (ε/M^{-1} cm^{-1})): 456 (1.03×10^3), 359 (1.51×10^3), 287 (3.71×10^3) and 249 (1.36×10^4). Anal. Calcd for $C_{11}H_{20}CoF_{12}N_3P_2$·NaCl: C, 21.96; H, 3.35; N, 6.99. Found: C, 21.68; H, 3.35; N, 7.15. The elemental analysis data best fit with one sodium chloride, which comes from the NaOH deprotonation of [9]aneN$_3$·3HCl. Cyclic voltammetry shows one irreversible one-electron reduction with $E^{\circ\prime} = -1.042$ V, $i_{pc}/i_{pa} = 2.291$, $\Delta E_p = 73$ mV versus Fc /Fc$^+$ ($i_{pc}/i_{pa} = 1.024$ and $\Delta E_p = 71$ mV).

2.3.6. Preparation of [Co(Cp*)([9]aneN$_3$))](PF$_6$)$_2$ (4)

A 100 mL round-bottom flask was charged with [9]aneN$_3$·3HCl (0.0602 g, 0.252 mmol) and EtOH (30 mL). To the mixture, 7.00 mL of dilute aqueous NaOH (0.1 M, 0.700 mmol) was added in 3 portions waiting 10–15 min between each addition. After the NaOH addition, the solution became homogeneous, and was slightly basic according to pH paper. To this solution, [Co(Cp*)(CO)(I)$_2$] (0.100 g, 0.210 mmol) was added and this solution was heated to reflux under N_2 for 2 h. The solution was cooled and $AgPF_6$ (0.123 g, 0.486 mmol) was added, immediately giving rise to a precipitate. The mixture was heated to reflux under N_2 for 30 min in the dark giving rise to a cherry red solution with a brown precipitate. Once cooled to room temperature, the mixture was filtered through celite plug and the filtrate was reduced to ~1 to 2 mL on the rotary evaporator. An orange product precipitated upon the addition of diethyl ether ~20 mL, which was collected by vacuum filtration and was dried *in vacuo*. (0.0657 g, 51% yield). ^{1}H NMR (CD_3NO_2, δ): 5.76 (3H, s, [9]aneN$_3$ N*H*) 3.37–2.73 (12H, m, [9]aneN$_3$ C*H*$_2$), 1.63 (15H, s, Cp* C*H*$_3$). ^{13}C{^{1}H} NMR (CD_3NO_2, δ): 93.4 (5C, s, Cp* *C*CH$_3$), 52.1 (6C, s, [9]aneN$_3$ *C*H$_2$), 9.1 (5C, s, Cp* *C*H$_3$). ^{31}P NMR (CD_3NO_2, δ): −144 (1P, m, *P*F$_6$). UV-Vis (acetonitrile, nm (ε/M^{-1} cm^{-1})): 482 (1.22×10^3), 305 (1.44×10^3) and 273 (1.93×10^4). Anal. Calcd for $C_{16}H_{30}CoF_{12}N_3P_2$·2H$_2$O: C, 29.60; H, 5.28; N, 6.47. Found: C, 29.35; H, 4.72; S, 6.49. Cyclic voltammetry shows one reversible one-electron reduction with $E^{\circ\prime} = -1.324$ V, $i_{pc}/i_{pa} = 1.042$, $\Delta E_p = 68$ mV versus Fc /Fc$^+$ ($i_{pc}/i_{pa} = 1.003$ and $\Delta E_p = 68$ mV).

2.4. X-ray crystallography data collection and processing

Single crystals of complexes **1**, **2**, and **4** suitable for diffraction were grown by diffusion of diethyl ether into a nitromethane solution of the appropriate complex. The crystal data, collection parameters and refinement criteria for these compounds can be found in Table 1. Crystals were mounted on the tip of a Bruker SPINE-pin mount and X-ray intensity data were measured at low temperature using an Oxford Cryosystems Desktop Cooler (200(2) K) for all structures with a graphite monochromated Mo kα radiation (λ = 0.71073 Å) on a Bruker SMART X2S Benchtop diffractometer. Integration, data reduction and scaling were carried out with the programs SAINT and SADABS in the Bruker APEX2 suite of software [40]. Each structure was solved (XS) using direct methods and refined using full matrix least squares refinement (SHELXL2017) within Olex2 [41–43]. A direct-methods solution was calculated that provided the non-hydrogen atoms from the E-map. All non-hydrogen atoms were refined with anisotropic displacement parameters. All of the hydrogen atoms in each structure were placed in ideal positions and refined as riding atoms. Refinement details for each structure are available in the Supplemental Material.

3. Results and discussion

3.1. Syntheses

The four heteroleptic complexes, [Co(Cp^R)([9]aneX$_3$)](PF$_6$)$_2$, where R = H, Cp or Me, Cp* and X = N, [9]aneN$_3$ or S, [9]aneS$_3$, are prepared by direct ligand substitution reactions from the starting complexes [Co(Cp^R)(CO)(I)$_2$] [38,39], and are stable both as a solid and in solution. For the metathesis reactions involving [9]aneS$_3$ (complexes **1** and **2**) it was found that tetra-*n*-butylammonium hexafluorophosphate works best due to the ethanol solubility of both the reacting salt and the by-

Table 1
Crystallographic data for [Co(Cp)([9]aneS$_3$)](PF$_6$)$_2$·CH$_3$NO$_2$ (**1**), [Co(Cp*)([9]aneS$_3$)](PF$_6$)$_2$·2CH$_3$NO$_2$ (**2**), and [Co(Cp*)([9]aneN$_3$)](PF$_6$)$_2$·CH$_3$NO$_2$ (**4**).

	(1)	(2)	(4)
Formula	$C_{12}H_{20}CoF_{12}NO_2P_2S_3$	$C_{18}H_{33}CoF_{12}N_2O_4P_2S_3$	$C_{17}H_{33}CoF_{12}N_4O_2P_2$
Habitat, color	Block, orange	Block, orange	Block, orange
Lattice type	Orthorhombic	Monoclinic	Triclinic
Space group	$P2_12_12_1$	$P2_1/c$	P-1
a, Å	8.3865(10)	19.305(3)	9.4662(8)
b, Å	15.502(2)	15.706(2)	9.6769(8)
c, Å	17.347(3)	10.4385(16)	16.1389(14)
α,°	90	90	72.980(3)
β,°	90	99.326(5)	87.684(3)
γ,°	90	90	81.519(3)
V (Å^3)	2255.3(5)	3123.2(8)	1398.2(2)
Z	4	4	2
Fwt, g mol^{-1}	655.34	786.51	674.33
D_c, g cm^{-3}	1.930	1.673	1.607
μ, (mm^{-1})	1.291	0.953	0.832
T (K)	200(2)	200(2)	200(2)
Reflections collected	23,483	31,491	26,408
Unique reflections	3980 (R_{int} = 0.0927)	5039 (R_{int} = 0.0495)	4957 (R_{int} = 0.0524)
Data, restraints, param.	3980/883/455	5039/1674/578	4957/802/501
R_1, wR_2 ($I > 2s(I)$)	0.0368, 0.0882	0.0448, 0.1130	0.0388, 0.0905
R_1, wR_2 (all data)	0.0420, 0.0911	0.0651, 0.1263	0.0500, 0.0965
Goodness-of-fit (F^2)	1.027	1.029	1.050
Largest diff. peak, hole, e Å^{-3}	0.38, −0.34	0.63, −0.41	0.38, −0.34
Flack parameter	0.574(13)	N/A	N/A

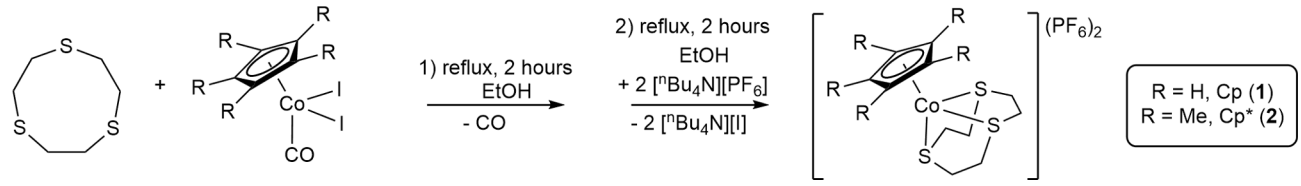

Scheme 1. Preparation of $[Co(Cp^R)([9]aneS_3)](PF_6)_2$ complexes.

product tetra-*n*-butylammonium iodide while the complexes $[Co(Cp^R)([9]aneS_3)](PF_6)_2$ precipitate upon formation (Scheme 1). However, with the $[9]aneN_3$ containing complexes **3** and **4**, $[Co(Cp^R)([9]aneN_3)](PF_6)_2$ remains soluble in ethanol. Therefore, silver(I) hexafluorophosphate was used in place of tetra-*n*-butylammonium hexafluorophosphate and the by-product silver(I) iodide precipitates readily in ethanol (Scheme 2) leaving **3** or **4** behind in solution. Furthermore, with the $[9]aneN_3$ complexes it was found the reaction works best when starting with the protonated $[9]aneN_3{\cdot}3HCl$ salt. The hydrochloride salt reacts with dilute aqueous sodium hydroxide to produce $[9]aneN_3$ *in situ*, and then an ethanol solution of $[Co(Cp^R)(CO)(I)_2]$ is transferred to the deprotonated ligand. The Co(III) complex $[Co(Cp^*)([9]aneS_3)]^{2+}$ has been synthesized previously as a perchlorate compound; however, only a ^1H NMR was reported for this complex along with the crystal structure [44]. Herein we report the full characterization of this complex including the single-crystal structure elucidated from X-ray diffraction as a hexafluorophosphate coordination compound.

3.2. Structural studies

The structures of $[Co(Cp)([9]aneS_3)](PF_6)_2$ (**1**), $[Co(Cp^*)([9]aneS_3)](PF_6)_2$ (**2**), and $[Co(Cp^*)([9]aneN_3)](PF_6)_2$ (**4**) were determined by single-crystal X-ray diffraction. A crystallographic summary is given in Table 1, selected bond distances and angles in Table 2, and structural perspectives are shown in Figs. 1–3. All three structures feature facial coordination of both the η^5-Cp^R ligand and the tridentate macrocycle to form a six-coordinate pseudo-octahedral geometry where the macrocycles have all three donor atoms orientated in an endodentate fashion in each of the complexes. The Co-Cp^R centroid and Co-$[9]aneX_3$ centroid show little deviation upon changing from either Cp to Cp* or $[9]aneS_3$ to $[9]aneN_3$.

The crystal structure of $[Co(Cp)([9]aneS_3)](PF_6)_2$ (**1**) exhibits an average Co—S bond length of 2.2218(16) Å, an average Co—C bond length of 2.07(2) Å, an average C—S bond length of 1.821(6) Å, and the average S—Co—S chelate angle is 91.55(6)° (Fig. 1). As shown in Fig. 1, the Cp ring of **1** is disordered, which was modeled as two coplanar cyclopentadienyl rings rotated approximately 24° from each other. These values are similar to the average Co—C bond length in cobaltocenium hexafluorophosphate (2.0128(16) Å) [45], which indicates that our model is reasonable. It has been suggested that the π-acidity of thioethers like $[9]aneS_3$ can play a role in their coordination chemistry through access to the C—S σ* orbitals, which can lead to C—S bond lengthening [37]. However, the average C—S bond length in **1** is statistically identical to free $[9]aneS_3$ (1.820(5) Å) [46], which suggests there is little to no π-backbonding present in **1**. Indeed, the Co—S and C—S average bond lengths in **1** show only negligible change when compared to the respective average Co—S and C—S bond lengths of 2.253(1) Å and 1.822(4) Å in $[Co([9]aneS_3)_2](ClO_4)_3$ [47]. Furthermore, the isostructural and isoelectronic complex $[Fe(Cp)([9]aneS_3)]^+$ has an average Fe—S and C—S bond length of 2.2077(19) Å and 1.832 (17) Å, respectively, and the slightly elongated C—S bond length

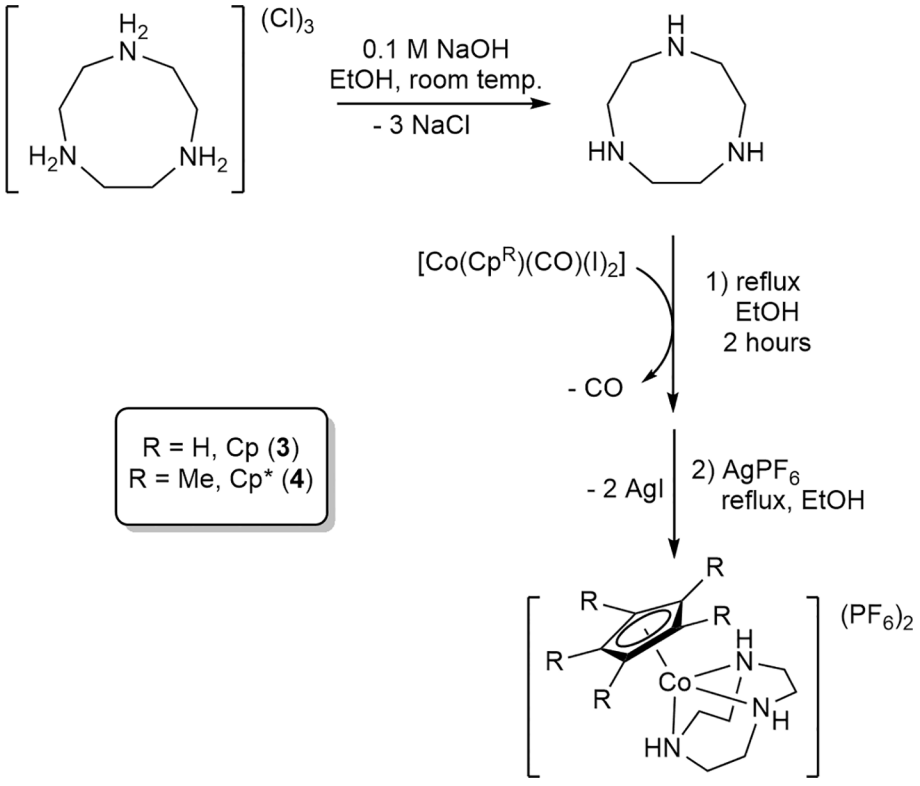

Scheme 2. Preparation of $[Co(Cp^R)([9]aneN_3)](PF_6)_2$ complexes.

Table 2
Selected bond distances (Å) and angles (°) with esds in parentheses for $[Co(Cp)([9]aneS_3)](PF_6)_2{\cdot}CH_3NO_2$ (**1**), $[Co(Cp^*)([9]aneS_3)](PF_6)_2{\cdot}2CH_3NO_2$ (**2**), and $[Co(Cp^*)([9]aneN_3)](PF_6)_2{\cdot}CH_3NO_2$ (**4**).

	(1)	(2)	(4)
Distances (Å)			
Co-X1	2.2241(15)	2.2137(12), 2.14(3)[c]	1.997(3), 1.967(14)[c]
Co-X2	2.2195(17)	2.2173(13), 2.11(3)	2.000(3), 1.892(15)
Co-X3	2.22164(17)	2.2120(13), 2.02(3)	1.983(3), 1.966(14)
Co-C1/C7[a]	2.108(19), 2.11(2)[b]	2.079(4)	2.077(2)
Co-C2/C8	2.039(15), 2.11(2)	2.075(4)	2.068(3)
Co-C3/C9	2.05(2), 2.11(4)	2.096(4)	2.075(3)
Co-C4/C10	2.074(16), 2.04(3)	2.073(4)	2.067(3)
Co-C5/C11	2.085(19), 2.01(3)	2.101(4)	2.073(3)
Co-[9]aneX$_3$ centroid	1.24636(15)	1.25523(15), 1.05953(12)[c]	1.25832(8), 1.19171(8)[c]
Co-Cp^R centroid	1.687(12), 1.6950(2)[b]	1.6985(2)	1.67921(11)
X-C[d]	1.821(6)	1.800(5)	1.480(6)
Angles (°)			
X1-Co-X2	91.09(6)	91.12(6), 95.6(13)[b]	83.87(13), 87.2(5)[b]
X2-Co-X3	91.85(6)	90.84(6), 99.1(14)	84.48(13), 86.7(5)
X3-Co-X1	91.73(6)	91.13(6), 95.3(14)	84.85(14), 85.05(5)

[a] The Cp ring was labeled C1–C5 for **1** and C7–C11 for **3** and **4** to help in modeling the disorder of the Cp ring (**1**) and the macrocycles (**3** and **4**).
[b] Includes both modeled Cp rings.
[c] Includes both modeled macrocycle rings.
[d] Average C-X bond length in either 1,4,7-trithiacyclononane (X = S) or 1,4,7-triazacyclononane (X = N).

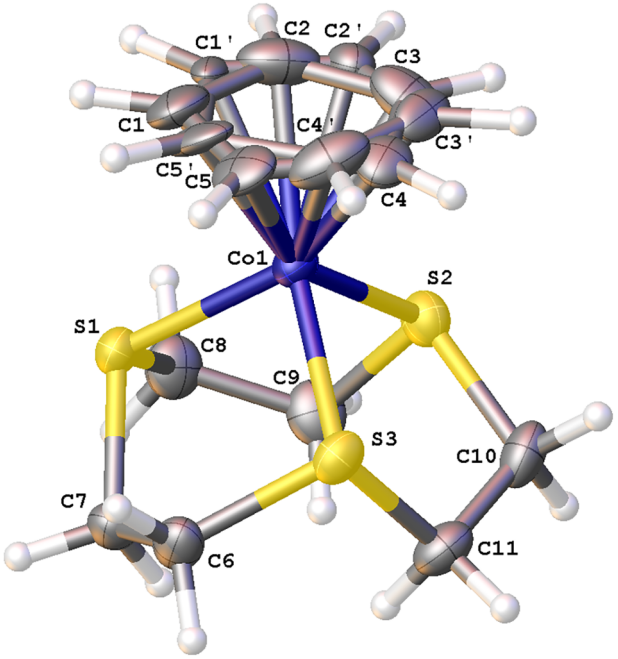

Fig. 1. Thermal ellipsoid perspective (50% probability) for the complex cation of **1**. A nitromethane solvate molecule and two hexafluorophosphate anions have been omitted for clarity. Both orientations of the Cp ring are shown.

suggests in the Fe(II) complex that the size and charge on the metal center play a key role in π-backbonding [13].

The crystal structure of $[Co(Cp^*)([9]aneS_3)](PF_6)_2$ (**2**) exhibits an average Co—S bond length of 2.15(2) Å, an average Co—C bond length of 2.085(4) Å, an average C—S bond length of 1.800(5) Å, and the average S—Co—S chelate angle is 93.8(4)° (Fig. 2). As shown in Fig. 2, the [9]aneS$_3$ of **2** is disordered, which was modeled as two [9]aneS$_3$ macrocycles rotated approximately 33° from each other about the Co—Cp* vector. The average Co—C bond length is 2.053(13) Å in pentamethylcobaltocenium hexafluorophosphate [48], and the average Co—S bond length is 2.253(1) Å in $[Co([9]aneS_3)_2](ClO_4)_3$ [47]. The Co—C and Co—S bond lengths in **2** are longer and shorter, respectively, when compared to **1** and the respective bis-homoleptic complexes. This suggests that the Cp* is a better σ-donor compared to Cp; however, the C—S bond length for the coordinated [9]aneS$_3$ does not lengthen from free ligand. The Co—C and Co—S bond lengths in **2** may be a result of sterics and not electronics (Cp* vs. Cp), and the disorder in the coordinated [9]aneS$_3$ cannot be discounted either. Metal size plays a key role when coordinated to the sulfurs on the [9]aneS$_3$ macrocycle as evidenced in the average S—M—S chelate angle change in the Group 9 triad for $[M(Cp^*)([9]aneS_3)](PF_6)_2$, M = Co (93.9(4)°) to M = Rh/Ir (88.3(3)°/87.8(2)°) [24].

The crystal structure of $[Co(Cp^*)([9]aneN_3)](PF_6)_2$ (**4**) exhibits an average Co—N bond length of 1.968(2) Å, an average Co—C bond length of 2.072(3) Å, and the average N—Co—N chelate angle is 84.5(3)°, which, as expected, is smaller than observed in **1** and **2** for the larger sulfur (Fig. 3). As shown in Fig. 3 the [9]aneN$_3$ of **4** is disordered, which was modeled as two [9]aneN$_3$ macrocycles rotated approximately 20° from each other about the Co—Cp* vector. The average Co—N bond length is 1.962(12) Å in $[Co([9]aneN_3)_2](ClO_4)_3$ [49], and the negligible change in the Co—C and Co—N bond lengths in **4** compared to the respective bis-homoleptic complexes suggests that both the Cp* and [9]aneN$_3$ behave similarly as σ-donor ligands. The average Co—C bond length shows negligible change between complexes **2** and **4**, which again suggests that the [9]aneS$_3$ ligand is acting as a σ-donor with Co(III) rather than a π-acceptor. As observed in **2**, the metal size impacts the coordination geometry as seen in the average N—M—N chelate angle in the Group 9 triad for $[M(Cp^*)([9]aneN_3)](PF_6)_2$, M = Co (84.5(3)°) to M = Rh/Ir (80.2(15)°/79.3(16)°) [24].

3.3. NMR spectroscopy

In the proton NMR spectra, the 12 methylene protons for the coordinated [9]aneN$_3$ or [9]aneS$_3$ ligands appear as a pair of broad resonances with a distinguishing AA′BB′ second order splitting pattern (see Supplemental Material for ^{1}H and ^{13}C NMR spectra for **1–4**), which is shifted downfield from free ligand. The magnetic inequivalence of the methylene protons arises from the different orientations of the protons with respect to the metal ion [50]. This same type pattern was observed in the homoleptic bis-[9]aneS$_3$ and [9]aneN$_3$ complexes with Co(III) [47]. There are few differences in the ^{1}H NMR spectra between Co(III)-Cp^R complexes involving the same macrocycle. In contrast, there are very noticeable distinctions when comparing the [9]aneS$_3$ and [9]aneN$_3$ complexes containing either Cp^R ring.

While it has been previously reported that the chemical dispersion for [9]aneX$_3$ mixed sandwich complexes is an indication of the π-

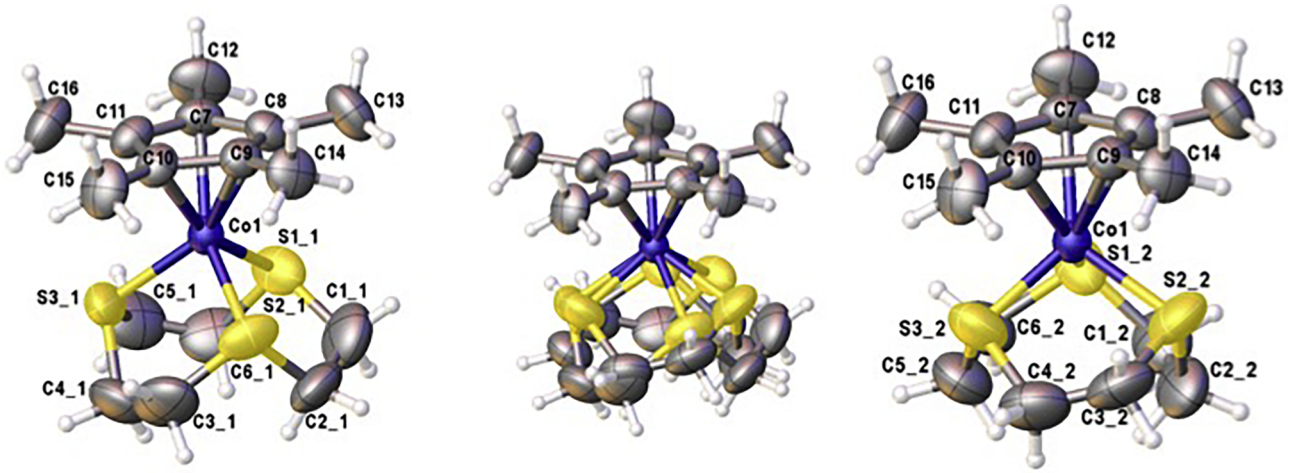

Fig. 2. Thermal ellipsoid perspective (50% probability) of **2**. Two nitromethane solvate molecules and two hexafluorophosphate anions have been omitted for clarity. The left and right structures show the individual orientations of the [9]aneS$_3$ ligand, and the center structure shows both [9]aneS$_3$ orientations rotated about the Co-Cp* vector.

accepting properties (or lack thereof) for the ligand [24], our compounds indicate that this observation can be more general and extended to both σ-donor and π-accepting ligands with the metal identity playing a key role. The [9]aneN$_3$ complexes (**3** and **4**) show a surprisingly large chemical dispersion for the methylene protons in their ^{1}H NMR spectra. The Cp complex (**3**) shows a separation of 0.74 ppm between the two sets of second order AA′BB′ multiplets while the Cp* complex (**4**) shows a separation of 0.64 ppm. This is compared to the separation being only 0.31 ppm for **1** (Cp/[9]aneS$_3$) and 0.18 ppm for **2** (Cp*/[9]aneS$_3$). Interestingly, the separation between the two multiplets is reversed from that observed for the previously reported isostructural [M(Cp*)([9]aneX$_3$)](PF$_6$)$_2$, where M = Rh or Ir and X = N or S, complexes [24]. The distinction between the multiplet dispersion separation in the two types of cyclononane macrocycles for the heteroleptic mixed sandwich complexes was proposed to arise from the differences in their donor/acceptor properties; specifically, the π-acidity of the thioether with the π-basic Rh(III) and Ir(III) ions. For the complexes reported herein with Co(III), the dispersion of the [9]aneN$_3$ methylene protons is greater and enhanced with Cp compared to Cp*. We propose that this too is likely attributable to differences in their donor/acceptor properties with the small, electron-deficient Co(III) preferring coordination with the σ-donor azaether. From these data, it appears that the greater dispersion of the AA′BB′ methylene protons for the coordinated macrocycle in a heteroleptic environment occurs when the coordinating properties match better with the identity of the metal. It should be noted that the splitting patterns for the bis-homoleptic [9]aneS$_3$ and [9]aneN$_3$ complexes of Co(III) are consistent with the mixed sandwich heteroleptic complexes reported herein [47].

The methylene carbon shift for the coordinated macrocycle is a singlet at 39 ppm and 41 ppm for **1** and **2**, respectively, and is shifted downfield slightly from the bis-homoleptic [9]aneS$_3$ complex. The methylene carbons of the coordinated macrocycle resonate as one singlet by ^{13}C{^{1}H} NMR at room temperature, which is due to a 1,4-metallotropic shift process that results in all 6 carbon atoms being equivalent [51,52]. The methylene resonance is at 54 ppm and 52 ppm for **3** and **4**, respectively, and shows no change from the bis-homoleptic [9]aneN$_3$ complex. Interestingly, the chemical shift of the ring carbons for the Cp/Cp* are highly dependent on the identity of the macrocycle. For complexes **3** and **4**, which contain [9]aneN$_3$, only a 1–2 ppm shift downfield from the homoleptic complexes [Co(Cp^R)$_2$](PF$_6$) is observed. However, for the [9]aneS$_3$ analogs, **1** and **2**, an 8–10 ppm shift downfield from the homoleptic complexes [Co(Cp^R)$_2$](PF$_6$) is observed. This trend was also observed with the Cp*Rh and Cp*Ir analogs [24], which is in agreement with all three metals within the Group 9 triad as opposed to the AA′BB′ dispersions of the coordinated macrocycles in the ^{1}H NMR being reversed with Co(III) vs. Rh(III)/Ir(III).

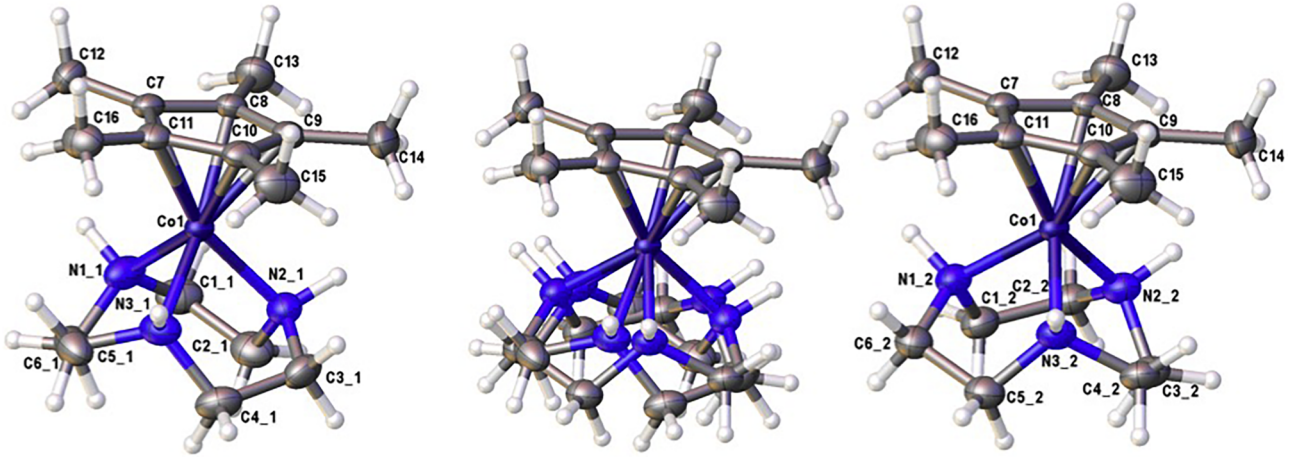

Fig. 3. Thermal ellipsoid perspective (50% probability) for the complex cation of **4**. A nitromethane solvate molecule and two hexafluorophosphate anions have been omitted for clarity. The left and right structures show the individual orientations of the [9]aneN$_3$ ligand, and the center structure shows both [9]aneN$_3$ orientations rotated about the Co-Cp* vector.

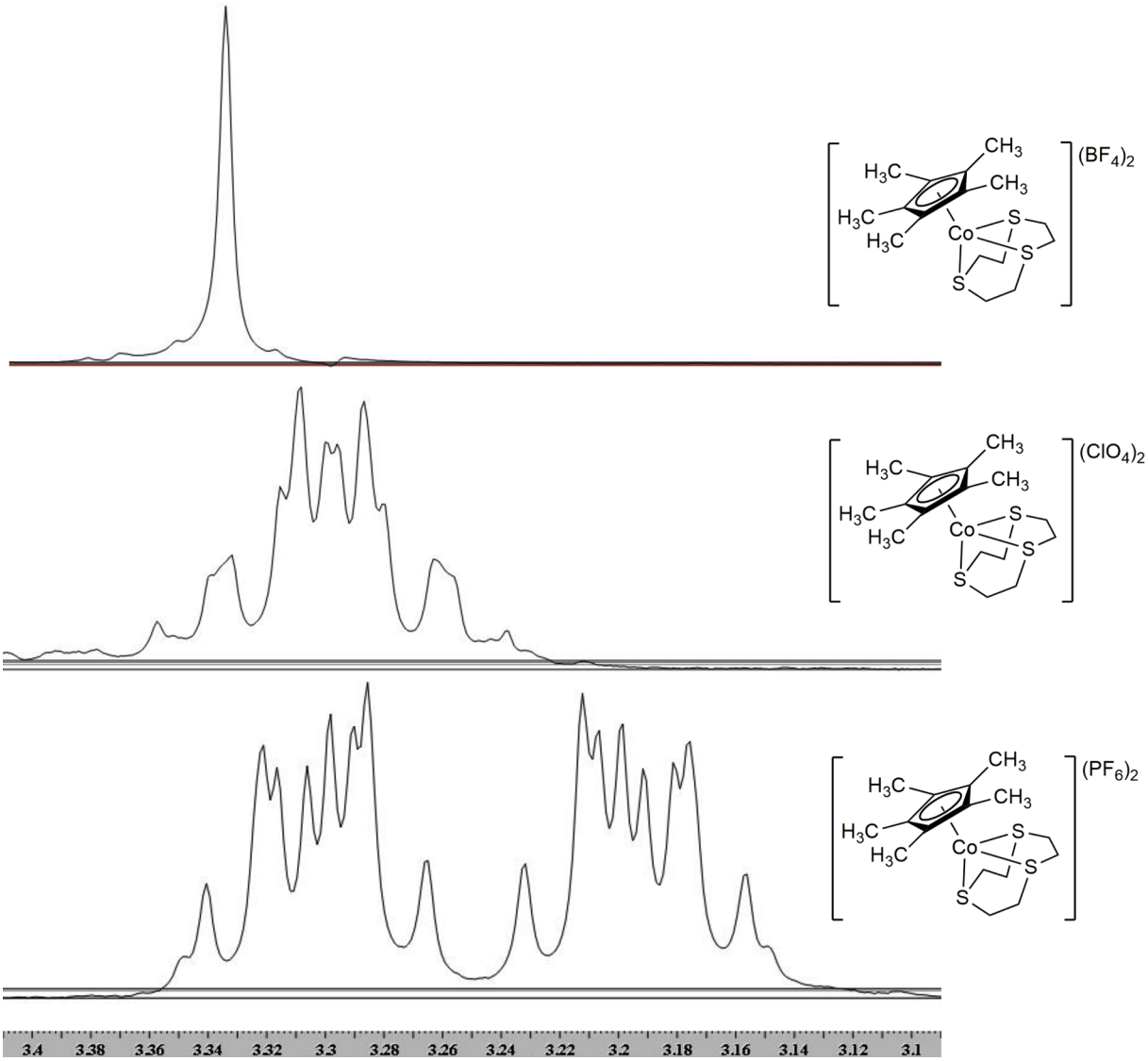

Fig. 4. ^{1}H NMR of [Co(Cp*)([9]aneS$_3$)](Y)$_2$ (**2**) complexes in CD_3NO_2, where Y = PF_6^-, ClO_4^-, or BF_4^-; at 25 °C only showing the [9]aneS$_3$ AA′BB′ dispersion (full spectral window is available in the Supplemental Material).

Outer sphere anion effects in related complexes of the type [Co(Cp)(P—P)(I)](Y), where P—P is a bidentate phosphane of the type $Ph_2P(CH_2)_nPPh_2$ with n = 1–4 and Y is I^-, PF_6^-, or BF_4^-, have been reported where the ^{1}H NMR chemical shift of the Cp is dependent on anion identity [53]. We had interest if similar contact ion pair effects would be present with our tridentate sulfur donor ligand, specifically for [Co(Cp*)([9]aneS$_3$)](Y)$_2$, where Y = PF_6^-, ClO_4^-, BF_4^-. Indeed, we observed the AA′BB′ dispersion range in the ^{1}H NMR for **2** to change from 0.20 ppm to 0.13 ppm to 0 ppm, upon changing Y from PF_6^- to ClO_4^- to BF_4^-, respectively (Fig. 4). This suggests a size dependence of the outer sphere anion and the nature of the AA′BB′ splitting of the coordinated macrocycle. In order to explore this, variable-temperature ^{1}H NMR spectroscopy was done with these three complexes (see Supplemental Material for additional NMR spectra). For the octahedral anion PF_6^- in CD_3NO_2, only a negligible reduction for the separation between the multiplets (0.08 ppm) was observed upon heating from 25 °C to 55 °C. Since the separation was already at 0.20 ppm at room temperature there was no need to look at lower temperatures. At the other size extreme, the smaller tetrahedral anion, Y = BF_4^-, showed a singlet between −10 °C and 35 °C for the methylene protons of the coordinated macrocycle in CD_3NO_2. For the other tetrahedral anion, Y = ClO_4^-, a fully reversible temperature dependence on the separation of the multiplets was observed. No change was observed upon going from 25 °C to 55 °C where the separation remained 0.13 ppm; however, upon cooling to −20 °C the dispersion increases to 0.16 ppm. Though the exact mechanism is unclear, the size of the outer sphere anion plays a clear role. Moreover, for the three anions that were studied, the medium-size perchlorate shows temperature dependence. In addition to the anion identity, solvent can play a role in the separation. For example, when Y = BF_4^- the coordinated macrocycle is no longer a singlet but showed the expected AA′BB′ splitting with a separation of 0.17 ppm between the two sets of multiplets at 20 °C in acetone-d_6, and does show some temperature dependence (see Supplemental Material).

3.4. Electrochemistry

The electrochemistry of the four trivalent metal complexes is dominated by a single reduction between −0.5 V and −1.6 V vs. Fc/Fc$^+$, which is assigned as the +3/+2 reduction of the metal (Table 3). This reduction matches the donating ability of the ligands that follow the order: **4**; −1.324 V < **3**; −1.042 V < **2**; −0.872 V < **1**; −0.582 V. The [9]aneS$_3$ complexes show a second quasi- or irreversible reduction between −1.5 and −1.9 V, which is assigned as the +2/+1

Table 3
Redox potentials, electronic spectra, and ligand field splitting data for [Co(Cp)([9]aneS$_3$)](PF$_6$)$_2$ (**1**), [Co(Cp*)([9]aneS$_3$)](PF$_6$)$_2$ (**2**), [Co(Cp)([9]aneN$_3$)](PF$_6$)$_2$ (**3**), [Co(Cp*)([9]aneN$_3$)](PF$_6$)$_2$ (**4**), [Co(Cp*)$_2$](PF$_6$), [Co(Cp)$_2$](PF$_6$), [Co([9]aneS$_3$)$_2$](ClO$_4$)$_3$, and [Co([9]aneN$_3$)$_2$](ClO$_4$)$_3$.

Complex	λ_{max}, nm (ε, L mol^{-1} cm^{-1})	Δ_o (cm^{-1})	B (cm^{-1})	$E^{o'}$ for Co^{3+}/Co^{2+} (V)[a]	Reference
[Co(Cp)([9]aneS$_3$)](PF$_6$)$_2$	432 (1.41 × 10^3), 363 (2.11 × 10^3), 305 (2.77 × 10^4), 246 (2.56 × 10^4)	2.40 × 10^4	294	−0.582 (reversible), −1.524 (quasi-reversible)[b]	This work
[Co(Cp*)([9]aneS$_3$)](PF$_6$)$_2$	440 (1.03 × 10^3), 359 (1.32 × 10^3), 300 (4.20 × 10^3)	2.36 × 10^4	308	−0.872 (quasi-reversible), −1.837 (irreversible)[b]	This work
[Co(Cp)([9]aneN$_3$)](PF$_6$)$_2$	456 (1.03 × 10^3), 359 (1.52 × 10^3), 287 (3.71 × 10^3), 249 (1.36 × 10^4)	2.29 × 10^4	409	−1.042 (irreversible)	This work
[Co(Cp*)([9]aneN$_3$)](PF$_6$)$_2$	482 (1.22 × 10^3), 305 (1.44 × 10^3), 273 (1.93 × 10^4)	2.05 × 10^4	1.02 × 10^3	−1.324 (reversible)	This work
[Co(Cp*)$_2$](PF$_6$)	341 (1.45 × 10^3)[e], 294 (4.12 × 10^4)	N/A	N/A	−1.525 (reversible)[c]	[55]
[Co(Cp)$_2$](PF$_6$)	405 (2 3 1), 300 (1.44 × 10^3), 262 (3.61 × 10^4)	2.59 × 10^4	617	−1.327 (reversible), −2.291 (irreversible)[b]	This work
[Co([9]aneS$_3$)$_2$](ClO$_4$)$_3$	476 (3 2 0)[e], 330 (2.20 × 10^4)	N/A	N/A	+0.42 (quasi- reversible), −0.48 (quasi-reversible)[b,d]	[52]
[Co([9]aneN$_3$)$_2$](ClO$_4$)$_3$	458 (1 0 0), 333 (89)	2.29 × 10^4	593	−0.41 (reversible)	[52]

[a] Values vs Fc/Fc$^+$ in acetonitrile, except as noted.
[b] Redox potential for Co^{2+}/Co^{1+} vs. Fc/Fc$^+$ in acetonitrile.
[c] Potential as reported vs. SCE in acetonitrile.
[d] Potential as reported vs. NHE in aqueous solution.
[e] Only a single *d-d* transition was observed or reported for [Co(Cp*)$_2$](PF$_6$) and [Co(Cp*)([9]aneS$_3$)](PF$_6$)$_2$, respectively.

reduction of the metal, at −1.524 V for **1** and −1.837 V for **2**. Direct comparisons to the homoleptic complexes [Co([9]aneX$_3$)$_2$](ClO$_4$)$_3$ and [Co(Cp*)$_2$](PF$_6$) should be viewed with caution as previous experiments were performed in aqueous solution (Table 3) [47,54,55]. However, the overall data trend does support the electron donation of the ligands following the order Cp* > Cp > [9]aneN$_3$ > [9]aneS$_3$, which agrees with what would be expected based on the σ-donor/ π-accepting properties of these particular ligands. The strongly electron-donating carbocyclic ligands destabilize the lower Co oxidation states, as does the macrocyclic [9]aneN$_3$, making reduction more difficult with complexes involving these ligands. Our observed reduction potentials for the +3/+2 couple of [Co(Cp^R)([9]aneX$_3$)](PF$_6$)$_2$ all fall nearly intermediate between those of the two homoleptic complexes, [Co(Cp^R)$_2$](PF$_6$) and [Co([9]aneX$_3$)$_2$](ClO$_4$)$_3$ even with [Co([9]aneX$_3$)$_2$](ClO$_4$)$_3$ and [Co(Cp*)$_2$](PF$_6$) being reported in either aqueous solution and referenced to NHE or in acetonitrile referenced to SCE, respectively. Of particular note is that the heteroleptic mixed sandwich complexes involving [9]aneS$_3$ show a second quasi- or irreversible reduction. The +2/+1 reduction is observed only in the [9]aneS$_3$ complexes, which includes the bis-homoleptic complex [Co([9]aneS$_3$)$_2$](ClO$_4$)$_3$ [47].

3.5. Electronic spectroscopy

As expected for a low-spin d^6 metal ion like Co(III), we observe two *d–d* electronic transitions for each of the heteroleptic mixed sandwich complexes (Table 3). These are assigned as the $^1A_{1g} \rightarrow {}^1T_{1g}$ and $^1A_{1g} \rightarrow {}^1T_{2g}$ transitions (based upon a pseudo-octahedral analysis), and occur in the range of 430–490 nm and 300–370 nm. Despite the approximate C_{3v} symmetry (assuming rapid Cp^R rotation around the Co center in solution), the general form of the electronic spectrum still resembles an octahedral complex. From the electronic spectrum of the mixed sandwich complexes, cobaltocenium hexafluorophosphate, and [Co([9]aneN$_3$)$_2$](ClO$_4$)$_3$, we calculated values of Δ_o and the Racah parameter B, which are shown in Table 3. An experimentally determined Δ_o value for [Co([9]aneN$_3$)$_2$](ClO$_4$)$_3$ has been determined to be 26,800 cm^{-1}, which is approximately 0.5 eV higher than what we calculate [49]. A second *d-d* transition was not observed for either [Co([9]aneS$_3$)$_2$](ClO$_4$)$_3$ or [Co(Cp*)$_2$](PF$_6$) [47]. The values of Δ_o decrease in the order of [Co(Cp)$_2$](PF$_6$); 25895 cm^{-1} > **1**; 24014 cm^{-1} > **2**; 23614 cm^{-1} > **3**; 22938 cm^{-1} > [Co([9]aneN$_3$)$_2$](ClO$_4$)$_3$; 22885 cm^{-1} > **4**; 20458 cm^{-1}. From these data, the Cp and the [9]aneS$_3$ result in the strongest ligands fields while the Cp* and [9]aneN$_3$ result in slightly smaller ligand fields. Thus, we suggest that the [Co(Cp*)$_2$](PF$_6$) and [Co([9]aneS$_3$)$_2$](ClO$_4$)$_3$ complexes be placed after **1** and before **2**, respectively, to complete this trend. This would result in the ligand field for Co(III) being strongest for Cp > [9]aneS$_3$ ~ Cp* > [9]aneN$_3$. The value of the interelectronic repulsion parameters, B, are consistent with a high degree of metal–ligand orbital mixing, for the sulfur containing complexes, and excluding the bis-Cp complex, follow the general order as Δ_o increases B decreases. One and two higher energy (< 300 nm) charge transfer transitions are observed in the Cp* and Cp complexes, respectively, regardless of the identity of the macrocycle.

4. Conclusions

Four heteroleptic mixed sandwich complexes containing Cp^R, the Group 9 transition metal ion Co(III), and the tridentate macrocycles [9]aneS$_3$ or [9]aneN$_3$ have been prepared. All four complexes are characterized in solution using ^{1}H and ^{13}C{^{1}H} NMR spectroscopy, and three complexes were structurally characterized by single-crystal X-ray diffraction. All show a pseudo-octahedral geometry formed by the facially coordinating tridentate macrocycle and the carbocyclic ligand. The average Co—C and Co—X bond lengths in the heteroleptic mixed sandwich complexes show little change from their respective bis-homoleptic complexes. In the ^{1}H NMR, the [9]aneS$_3$ complexes displayed an AA′BB′splitting pattern of their methylene protons with a dispersion between the two multiplet sets that is influenced by the size of the outer sphere anion. That same dispersion was noticeably smaller in the [9]aneS$_3$ complexes compared to [9]aneN$_3$, and is proposed to arise from the preference of the hard acid Co(III) for the hard base, [9]aneN$_3$. The σ-donor macrocycle [9]aneN$_3$ shows only one reduction potential, assigned as the +3/+2, centered between −1.0 and −1.3 V vs. Fc/Fc$^+$ and is closer to −1.3 V for the more electron rich Cp*. In contrast, the π-accepting property of the [9]aneS$_3$ macrocycle allows for two reduction potentials with the first reduction being more favorable than the [9]aneN$_3$ analogs and the second, assigned as the +2/+1 reduction, centered between −1.5 and −1.8 V vs. Fc/Fc$^+$ and again is closer to −1.8 V for the more electron rich Cp*. Taking together, our results suggest: the octahedral ligand field around the Co(III) center increasing in the order Cp > [9]aneS$_3$ ~ Cp* > [9]aneN$_3$, the electron donating ability of the ligands themselves increases in the order Cp* > Cp > [9]aneN$_3$ > [9]aneS$_3$, in the solid-state all four ligands behave similarly as σ-donors while the electrochemistry and electronic spectroscopy highlights the differences between the σ-donor/hard-base [9]aneN$_3$ and the π-acid/soft base [9]aneS$_3$ macrocycles.

Acknowledgments

Acknowledgements are made to Research Corporation for a Cottrell College Science Award (23288) and the National Science Foundation MRI Program (CHE-0951711) for purchase of the Bruker SMART X2S single-crystal X-ray diffractometer at the University of Tennessee at Chattanooga, and the Grote Chemistry Fund at UTC. We would like to thank Professor Gregory J. Grant (UTC, Emeritus) for useful discussions on [9]aneS$_3$ and [9]aneN$_3$ chemistry. We would like to thank Dr. Bruce Noll (Bruker AXS), Dr. Allen Oliver (Notre Dame University) and Dr. Amy Sarjeant (Cambridge Crystallographic Data Centre) for useful discussions on the crystal structures of complex **1** and **2**.

Appendix A. Supplementary data

Supplementary data to this article can be found online at https://doi.org/10.1016/j.ica.2018.08.058.

References

[1] M.A. Bennett, A.C. Willis, L. Yoong Goh, W. Chen, Polyhedron 15 (1996) 3559–3567.
[2] M.A. Bennett, L.Y. Goh, A.C. Willis, J. Am. Chem. Soc. 118 (1996) 4984–4992.
[3] A.J. Blake, M.A. Halcrow, M. Schröder, J. Chem. Soc., Chem. Commun. (1991) 253–256.
[4] A.J. Blake, M.A. Halcrow, M. Schröder, J. Chem. Soc., Dalton Trans. (1994) 1631–1639.
[5] J.C. Cannadine, A.F. Hill, A.J.P. White, D.J. Williams, J.D.E.T. Wilton-Ely, Organometallics 15 (1996) 5409–5415.
[6] P. Chaudhuri, K. Wieghardt, Progress in Inorganic Chemistry, Wiley, New York, 1987.
[7] S.R. Cooper, S.C. Rawle, Struct. Bond. (Berlin) 72 (1990) 1.
[8] A.F. Hill, J.D.E.T. Wilton-Ely, Organometallics 16 (1997) 4517–4518.
[9] J.P. Lee, C.L. Keller, A.A. Werlein, D.E. Janzen, D.G. VanDerveer, G.J. Grant, Organometallics 31 (2012) 6505–6513.
[10] A.J. Welch, A.S. Weller, Inorg. Chem. 35 (1996) 4548–4554.
[11] G.J. Karahalis, A. Thangavel, B. Chica, J. Bacsa, R.B. Dyer, C.C. Scarborough, Inorg. Chem. 55 (2016) 1102–1107.
[12] A. Thangavel, M. Wieliczko, J. Bacsa, C.C. Scarborough, Inorg. Chem. 52 (2013) 13282–13287.
[13] A.J. Blake, R.D. Crofts, G. Reid, M. Schröder, J. Organomet. Chem. 359 (1989) 371–378.
[14] L.Y. Goh, M.E. Teo, S.B. Khoo, W.K. Leong, J.J. Vittal, J. Organomet. Chem. 664 (2002) 161–169.
[15] G.J. Grant, T. Salupo-Bryant, L.A. Holt, D.Y. Morrissey, M.J. Gray, J.D. Zubkowski, E.J. Valente, L.F. Mehne, J. Organomet. Chem. 587 (1999) 207–214.
[16] M. Green, M. Draganjac, Y. Jiang, A.W. Cordes, J. Chem. Crystallogr. 29 (1999) 273–276.
[17] R.Y.C. Shin, M.E. Teo, W.K. Leong, J.J. Vittal, J.H.K. Yip, L.Y. Goh, R.D. Webster, Organometallics 24 (2005) 1483–1494.
[18] K. Brandt, W.S. Sheldrick, J. Chem. Soc., Dalton Trans. (1996) 1237–1243.
[19] A. Hayashi, K. Nakajima, M. Nonoyama, Polyhedron 16 (1997) 4087–4095.
[20] M.N. Bell, A.J. Blake, R.M. Christie, R.O. Gould, A.J. Holder, T.I. Hyde, M. Schröder, L.J. Yellowless, J. Chem. Soc., Dalton Trans. (1992) 2977–2986.
[21] R.Y.C. Shin, M.A. Bennett, L.Y. Goh, W. Chen, D.C.R. Hockless, W.K. Leong, K. Mashima, A.C. Willis, Inorg. Chem. 42 (2003) 96–106.
[22] R. Wang, T.A. Eberspacher, T. Hasegawa, V. Day, D.C. Ware, H. Taube, Inorg. Chem. 40 (2001) 593–600.
[23] H.-J. Küppers, K. Wieghardt, S. Steenken, B. Nuber, J. Weiss, Z. Anorg. Allg. Chem. 573 (1989) 43–62.
[24] G.J. Grant, J.P. Lee, M.L. Helm, D.G. VanDerveer, W.T. Pennington, J.L. Harris, L.F. Mehne, D.W. Klinger, J. Organomet. Chem. 690 (2005) 629–639.
[25] L. Ackermann, J. Org. Chem. 79 (2014) 8948–8954.
[26] P.J. Chirik, Acc. Chem. Res. 48 (2015) 1687–1695.
[27] T.P. Brewster, N.M. Rezayee, Z. Culakova, M.S. Sanford, K.I. Goldberg, ACS Catal. 6 (2016) 3113–3117.
[28] W.D. Jones, F.J. Feher, J. Am. Chem. Soc. 106 (1984) 1650–1663.
[29] J.D. Lawrence, M. Takahashi, C. Bae, J.F. Hartwig, J. Am. Chem. Soc. 126 (2004) 15334–15335.
[30] C. Song, C. Yang, H. Zeng, W. Zhang, S. Guo, J. Zhu, Org. Lett. 20 (2018) 3819–3823.
[31] R. Mandal, B. Emayavaramban, B. Sundararaju, Org. Lett. 20 (2018) 2835–2838.
[32] S. Nakanowatari, R. Mei, M. Feldt, L. Ackermann, ACS Catal. 7 (2017) 2511–2515.
[33] J.K. Pagano, J.P.W. Stelmach, R. Waterman, Dalton Trans. 44 (2015) 12074–12077.
[34] Z. Zhang, S. Han, M. Tang, L. Ackermann, J. Li, Org. Lett. 19 (2017) 3315–3318.
[35] T.R. Cundari, T.V. Grimes, T.B. Gunnoe, J. Am. Chem. Soc. 129 (2007) 13172–13182.
[36] S.M. Bellows, T.R. Cundari, W.D. Jones, Organometallics 34 (2015) 4032–4038.
[37] G.E.D. Mullen, T.F. Fässler, M.J. Went, K. Howland, B. Stein, P.J. Blower, J. Chem. Soc., Dalton Trans. (1999) 3759–3766.
[38] R.B. King, Inorg. Chem. 5 (1966) 82–87.
[39] S.A. Frith, J.L. Spencer, Inorg. Syn. 28 (1990) 273–279.
[40] APEX2,, Bruker AXS Inc, Madison Wisconsin, USA, 2005.
[41] O.V. Dolomanov, L.J. Bourhis, R.J. Gildea, J.A.K. Howard, H. Puschmann, J. Appl. Crystallogr. 42 (2009) 339–341.
[42] G. Sheldrick, Acta Cryst Sect. A 71 (2015) 3–8.
[43] G. Sheldrick, Acta Cryst. Sec. C 71 (2015) 3–8.
[44] H.-J. Kim, J.H. Jeong, Y. Do, Bull. Korean Chem. Soc. 13 (1992) 463–465.
[45] D. Braga, L. Scaccianoce, F. Grepioni, S.M. Draper, Organometallics 15 (1996) 4675–4677.
[46] R.S. Glass, G.S. Wilson, W.N. Setzer, J. Am. Chem. Soc. 102 (1980) 5068–5069.
[47] H.J. Kueppers, A. Neves, C. Pomp, D. Ventur, K. Wieghardt, B. Nuber, J. Weiss, Inorg. Chem. 25 (1986) 2400–2408.
[48] D. Braga, O. Benedi, L. Maini, F. Grepioni, J. Chem. Soc., Dalton Trans. (1999) 2611–2617.
[49] Q. Wang, S. Yan, D. Liao, Z. Jiang, P. Cheng, X. Leng, H. Wang, J. Mol. Struct. 608 (2002) 49–53.
[50] G.J. Grant, Dalton Trans. 41 (2012) 8745–8761.
[51] G.J. Grant, C.G. Brandow, D.F. Galas, J.P. Davis, W.T. Pennington, E.J. Valente, J.D. Zubkowski, Polyhedron 20 (2001) 3333–3342.
[52] H. Nikol, H.B. Burgi, K.I. Hardcastle, H.B. Gray, Inorg. Chem. 34 (1995) 6319–6322.
[53] Q.B. Bao, S.J. Landon, A.L. Rheingold, T.M. Haller, T.B. Brill, Inorg. Chem. 24 (1985) 900–908.
[54] K. Wieghardt, W. Schmidt, W. Herrmann, H.J. Kueppers, Inorg. Chem. 22 (1983) 2953–2956.
[55] J.R. Aranzaes, M.-C. Daniel, D. Astruc, Can. J. Chem. 84 (2006) 288–299.